2009 IEEE International Conference on Robotics and Automation
Kobe International Conference Center
Kobe, Japan, May 12-17, 2009

Person identification from human walking sequences using affine moment invariants

Yumi Iwashita and Ryo Kurazume

Abstract— **This paper proposes a new person identification method using physiological and behavioral biometrics. Various person recognition systems have been proposed so far, and one of the recently introduced human characteristics for the person identification is gait. Although the shape of one's body has not been considered much as a characteristic, it is closely related to gait and it is difficult to disassociate them. So, the proposed technique introduces a new hybrid biometric, combining body shape (physiological) and gait (behavioral). The new biometric is the full spatio-temporal volume carved by a person who walks. In addition to this biometric, we extract unique biometrics in individuals by the following way: creating the average image from the spatio-temporal volume and forming the new spatio-temporal volume from differential images which are created by subtracting an average image from original images. Affine moment invariants are derived from these biometrics, and classified by a support vector machine. We used the leave-one-out cross validation technique to estimate the correct classification rate of 94 %.**

I. Introduction

Person recognition systems have been used for a wide variety applications, such as secure access to buildings, computer systems, automated teller machines (ATMs). For reliable personal recognition systems, biometrics have received growing interest. These include physiological biometrics, related to the shape of the body, the oldest of which are the fingerprints; and the behavioral biometrics, related to the behavior of a person, the first of which used was the signature. Several biometric recognition systems are available in the market. However, these systems need special equipment and require interaction with or cooperation of the subject.

One of the recently introduced human characteristics that are expected to overcome these limitations is gait [1] [10]. Gait is the peculiar way one walks and is a complex spatio-temporal biometric. Gait recognition has the advantage of being unobtrusive because body-invasive sensing is not needed to capture gait information. Moreover, gait recognition has the extra advantage that it may be performed from a distance.

One of the other characteristics that has not been considered much is the shape of one's body. This is probably because the shape of the body changes with time and with clothing. However, it is difficult to disassociate body shape from gait. So, this paper introduces a new hybrid biometric, combining body shape (physiological) and gait (behavioral). When a person walks, she/he carves a specific volume in the spatio-temporal domain. It is the shape of this volume we wish to consider as a biometric. In addition to this biometric, we consider another biometric, that is, the average image obtained from the spatio-temporal volume. Moreover, for emphasizing the difference of features in individuals, we form a new spatio-temporal volume from new differential images which are created by subtracting an average image from original images. In this paper we propose a novel person identification method which utilizes the full spatio-temporal volume, its average image, and the new spatio-temporal volume.

This paper is organized as follows. Section 2 is a brief literature survey on the identification of individuals using gait. Research that considers the spatio-temporal shapes created by a walking person is reviewed in section 2.2. However none of these papers considers the full volumes as potential biometrics. Section 3 describes the methodology we shall use in this paper. Section 4 describes the data we shall use and the experiments performed. Our results and conclusions are presented in section 5.

II. Literature survey on gait as a biometric

For person identification from their gait, several approaches have been proposed. They may be mostly classified into two classes, model-based and appearance-based approaches.

A. Model-based approaches

A model-based approach recovers explicit features describing gait dynamics, such as stride dimensions and the kinematics of joint angles. Bouchrika and Nixon [11] described spatial model templates for human gait in a parameterized form using Fourier descriptors. The positions of the joints of walking people were extracted by using the Hough Transform.

Cunado et al. [2] extracted the motion of the thigh, and defined their gait signature by Fourier analysis. Yam et al. [3] extended the system [2] to handle walking as well as running people. They extracted the motion of the hip, the thigh, and the lower leg by temporal template matching. Phase-weighted Fourier description gait signatures were derived from the extracted movements.

Urtasun and Fua [12] introduced a model composed of implicit surfaces attached to an articulated skeleton. The motion of people was tracked by using the 3D model and clusters of 3D points captured by a stereo camera. By using the 3D model, they increased the robustness to a changing view direction. Lee and Grimson [13] introduced

Y. Iwashita and R. Kurazume are with Graduate Faculty of Information Science and Electrical Engineering, Kyushu University, Motooka, Nishi-ku, Fukuoka 819-0395, Japan yumi, kurazume@is.kyushu-u.ac.jp

gait representation based on moments extracted from orthogonal view video silhouettes. Their gait appearance feature vector comprised parameters of moment features of image regions. Seven ellipses were fitted to different parts of the binarized silhouette of the person and the parameters of these ellipses, such as location of their centroids, eccentricities, etc., were used as features to represent the gait of the person. BenAbdelkader et al. [14] used stride and cadence for the identification of people. The person's identity was defined based on parametric Bayesian classification of the cadence and stride feature vector. From their experiments, the variation in stride length with cadence was found to be linear and unique for different people.

B. Appearance-based approaches

Appearance-based approaches directly extract parameters from images without assuming a model of the human body and its motion. This approach characterizes body movement by the statistics of the spatio-temporal (XYT) patterns generated in the image sequences by the walking person. Here, the XYT patterns are formed by piling up frames in an image sequence as shown in Fig.1. There are many ways of extracting XYT patterns from the image sequences of a walking person.

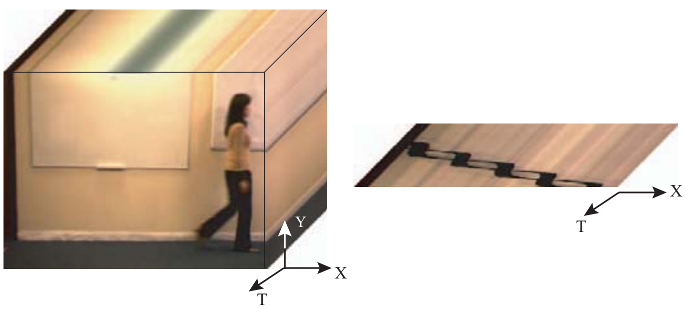

(a) XYT image sequence volume (b) Braided pattern in the XT-slice taken at the ankle

Fig. 1. XYT image sequence volume.

The simplest approach is to use the sequence of binary silhouettes spanning one gait cycle and scaled to a certain uniform size [4]. Murase and Sakai [4] proposed a template matching method in the parametric eigenspace that was created from images. Sarker et al. [5] proposed a baseline algorithm of gait recognition, which estimated the silhouettes by background subtraction and performed recognition by spatio-temporal correlation of silhouettes. Collins et al. [15] used silhouettes corresponding to certain gait poses only. Liu et al. [16] adopted dynamics-normalized shape cues with a population HMM which emphasize difference in stance shapes between subjects and suppresses differences for the same subject under different conditions.

Other methods use a signature of the silhouette by collapsing the XYT data into a more terse 1D or 2D signal, such as vertical projection histograms (XT), and horizontal projection histograms (YT) [17]. Niyogi and Adelson [17] extracted XT sheets that encoded the person's inner and outer bounding contours detected by fitting 'snakes'. Similarly, Liu et al. [18] extracted the XT and YT projections of the binary silhouettes. They used a frieze pattern to represent gait motion, that is a pattern created by summing up the white pixels of a binarized image of a gait along the rows and columns of an image. BenAbdelkader et al. [19] characterized gait in terms of a 2D signature computed directly from the sequence of silhouettes. The signature consisted of self-similarity plots (SSP), defined as the correlation of all pairs of images in the sequence. Han et al. used the gait energy image (GEI) which is based on the average image [6].

Little and Boyd [7] used optical flow instead of binary silhouettes. They fitted an ellipse to the dense optical flow of the person's motion, then computed thirteen scalar features consisting of first- and second-order moments of this ellipse. Twelve measurements were provided from thirteen features.

III. METHODOLOGY

In this section, we describe the methodology we use in this paper. Here, we assume that a target region in an image sequence is extracted.

A. Biometrics from human walking sequences

In the proposed method, we consider three biometrics, that is, the full spatio-temporal volume carved by a person who walks, the average image from the spatio-temporal volume, and the new spatio-temporal volume which is created by the average image and original images. The above biometrics are explained in details. Firstly, Fig. 1 (a) shows the 3D volume in the spatio-temporal (XYT) domain, and it is formed by piling up the target region in the image sequences of one gait cycle, which is used to partition the sequences for the 3D volume. One gait cycle is a fundamental unit to describe the gait during ambulation, which occurs from the time when the heel of one foot strikes the ground to the time at which the same foot contacts the ground again. In this paper, we assume that the 3D volume consists of a number of small voxels.

Next, the average image $I^{average}(x, y)$ is defined as follows:

$$I_i^{average}(x, y) = \frac{1}{T_i} \sum_{t=1}^{T_i} I_i(x, y, t), \quad (1)$$

where T is the number of frames in one gait cycle and $I(x, y, t)$ represents the density of the voxels at time t.

Finally, for emphasizing the difference of features in individuals, we create new images by subtracting the average image from the original images, and then the new spatio-temporal volume is formed. Here, the average image $I^{average}$ is defined as follows:

$$I^{average}(x, y) = \frac{1}{\sum_{i=1}^{N} T_i} \sum_{i=1}^{N} \sum_{t=1}^{T_i} I_i(x, y, t), \quad (2)$$

where N is the number of subjects. New images $I_i^{new}(x, y, t)$ are given by

$$I_i^{new}(x, y, t) = max(0, I_i(x, y, t) - I^{average}(x, y)). \quad (3)$$

Figure2 (a) shows the average image, and Fig.2 (b) shows an example of the differential images. For characterizing these 2D average images and 3D volumes, we consider the 2D and 3D affine moment invariants as features.

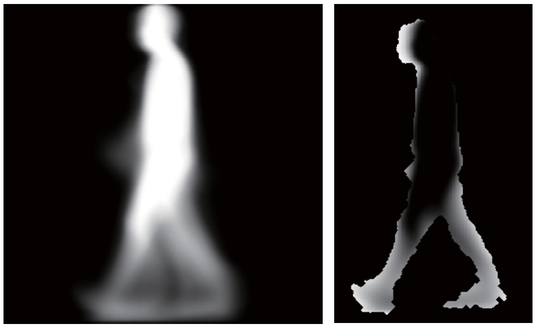

(a) An average image (b) An example a new image

Fig. 2. An average image and an example of differential images.

B. 2D and 3D affine moment invariants

In this section, we introduce the 2D and 3D affine moment invariants. Affine moment invariants are moment-based descriptors, which are invariant under a general affine transform. The moments describe shape properties of an object as it appears.

For an image $I(x, y)$ the 2D moment of order $(p+q)$ of an object O is given by

$$\mu_{pq} = \iint_{(x,y)\in O} x^p y^q I(x, y) dx dy. \tag{4}$$

The discrete version of Eq.4 is written as

$$\mu_{pq} = \sum\sum\nolimits_{(x,y)\in O} x^p y^q I(x, y). \tag{5}$$

The center of gravity of an object in the image can be determined from the zeroth and the first-order moments by

$$x_g = \frac{\mu_{10}}{\mu_{00}}, \qquad y_g = \frac{\mu_{01}}{\mu_{00}}. \tag{6}$$

Centralized moments are computed by using the coordinates x_g and y_g:

$$\mu_{pq} = \sum\sum\nolimits_{(x,y)\in O} (x - x_g)^p (y - y_g)^q I(x, y). \tag{7}$$

Six affine moment invariants are listed below [8].

$$\begin{aligned}
I_1 &= \frac{1}{\mu_{00}^4}(\mu_{20}\mu_{02} - \mu_{11}^2) \\
I_2 &= \frac{1}{\mu_{00}^{10}}(\mu_{30}^2\mu_{03}^2 - 6\mu_{30}\mu_{21}\mu_{12}\mu_{03} + 4\mu_{30}\mu_{12}^3 \\
&\quad +4\mu_{03}\mu_{21}^3 - 3\mu_{21}^2\mu_{12}^2) \\
I_3 &= \frac{1}{\mu_{00}^7}(\mu_{20}(\mu_{21}\mu_{03} - \mu_{12}^2) - \mu_{11}(\mu_{30}\mu_{03} \\
&\quad -\mu_{21}\mu_{12}) + \mu_{02}(\mu_{30}\mu_{12} - \mu_{21}^2)) \\
I_4 &= \frac{1}{\mu_{00}^{11}}(\mu_{20}^3\mu_{03}^2 - 6\mu_{20}^2\mu_{11}\mu_{12}\mu_{03} \\
&\quad -6\mu_{20}^2\mu_{02}\mu_{21}\mu_{03} + 9\mu_{20}^2\mu_{02}\mu_{12}^2 \\
&\quad +12\mu_{20}\mu_{11}^2\mu_{21}\mu_{03} + 6\mu_{20}\mu_{11}\mu_{02}\mu_{30}\mu_{03} \\
&\quad -18\mu_{20}\mu_{11}\mu_{02}\mu_{21}\mu_{12} - 8\mu_{11}^3\mu_{30}\mu_{03} \\
&\quad -6\mu_{20}\mu_{02}^2\mu_{30}\mu_{12} + 9\mu_{20}\mu_{02}^2\mu_{21}^2 \\
&\quad +12\mu_{11}^2\mu_{02}\mu_{30}\mu_{12} - 6\mu_{11}\mu_{02}^2\mu_{30}\mu_{21} \\
&\quad +\mu_{02}^3\mu_{30}^2) \\
I_5 &= \frac{1}{\mu_{00}^6}(\mu_{40}\mu_{04} - 4\mu_{31}\mu_{13} + 3\mu_{22}^2) \\
I_6 &= \frac{1}{\mu_{00}^9}(\mu_{40}\mu_{04}\mu_{22} + 2\mu_{31}\mu_{22}\mu_{13} \\
&\quad -\mu_{40}\mu_{13}^2 - \mu_{04}\mu_{13}^2 - \mu_{22}^3)
\end{aligned} \tag{8}$$

For a 3D space in which $I(x, y, t)$ represents the density of the voxels, the 3D moment of order $(p+q+r)$ of a 3D object O is given by the same procedure with 2D centralized moments.

$$\begin{aligned}
\mu_{pqr} &= \sum\sum\sum\nolimits_{(x,y,t)\in O} \\
&\quad (x - x_g)^p (y - y_g)^q (t - t_g)^r I(x, y, t),
\end{aligned} \tag{9}$$

where x_g, y_g and t_g are the coordinates of the center of gravity of an object in the 3D space.

Six 3D affine moment invariants are given in [9] [20], and two of them are listed below. For the rest of them, refer to [20] because of their long formulae.

$$\begin{aligned}
I_1 &= \frac{1}{\mu_{000}^5}(\mu_{200}\mu_{020}\mu_{002} + 2\mu_{110}\mu_{101}\mu_{011} \\
&\quad -\mu_{200}\mu_{011}^2 - \mu_{020}\mu_{101}^2 - \mu_{002}\mu_{110}^2) \\
I_2 &= \frac{1}{\mu_{000}^7}(\mu_{400}(\mu_{040}\mu_{004} + 3\mu_{022}^2 - 4\mu_{013}\mu_{031}) \\
&\quad +3\mu_{202}(\mu_{040}\mu_{202} - 4\mu_{112}\mu_{130} + 4\mu_{121}^2) \\
&\quad +12\mu_{211}(\mu_{022}\mu_{211} + \mu_{103}\mu_{130} - \mu_{031}\mu_{202} \\
&\quad -\mu_{112}\mu_{121}) + 4\mu_{310}(\mu_{031}\mu_{103} - \mu_{004}\mu_{130} \\
&\quad +3\mu_{013}\mu_{121} - 3\mu_{022}\mu_{112}) + 3\mu_{220}(\mu_{004}\mu_{220} \\
&\quad +2\mu_{022}\mu_{202} + 4\mu_{112}^2 - 4\mu_{013}\mu_{211} - 4\mu_{121}\mu_{103}) \\
&\quad +4\mu_{301}(\mu_{013}\mu_{130} - \mu_{040}\mu_{103} + 3\mu_{031}\mu_{112} \\
&\quad -3\mu_{022}\mu_{121}))
\end{aligned} \tag{10}$$

In the proposed method, we extract 2D affine moment invariants from the average image and 3D affine moment invariants from the full spatio-temporal volume of each subject at first, and the classifier is trained by using the training data sets. Then in the identification phase, the same affine moment invariants are extracted from the spatio-temporal volume and its average image, and the subject is identified by the classifier.

IV. Experiments

In this section we describe the experiments. In our experiments, we used a gait database collected by the University of Southampton [21]. The database contains 140 raw image sequences and foreground masks, which contains 140 video sequences, which contain 20 different subjects with 7 sequences for every subject. Figure 3 shows an example entry from the database.

Moreover, we describe the extended method with the aim of obtaining detailed features of the spatio-temporal volume. This method makes explicit the movement and shape of the arms from those of the legs, since different people move their arms differently when they walk. To extract these features, we divide the spatio-temporal volume into upper and lower volumes.

A. Experiments with the spatio-temporal volume and the average image

We carried out four experiments, and the experimental conditions are as follows: (Exp. A) the binarized spatio-temporal volume, (Exp. B) the average image from the spatio-temporal volume, (Exp. C) the new spatio-temporal volume created from the differential images, and (Exp. D) the average image and the new spatio-temporal volume. In our experiments, the support vector machine (SVM) and the k-nearest neighbour classification were applied to the affine moment invariants as the classifier. We used the leave-one-out cross validation to estimate the classification error rate.

In the first experiment the 3D affine moment invariants are used for the classification. Figure 4 shows the first two affine moment invariants used for 10 out of the 20 subjects and their whitened affine moment invariants. Here, data-specific variation can be removed by whitening. The resultant correct classification rate using the SVM and knn were 75 % and 69 %, respectively.

In the second experiment we used the 2D affine moment invariants. Figure 2 (a) shows an example of the average images. Here, the images are properly aligned and scaled to a uniform height before calculating the average image. The resultant correct classification rate using the SVM and knn were 92 % and 89 %, respectively. From this experiment, we could say that the average images show better performance for each person than the binary spatio-temporal volumes.

In the next experiment we used the the 3D affine moment invariants of the new spatio-temporal volume, which are created for emphasizing the difference of features in individuals. The resultant correct classification rate using the SVM and knn were 84 % and 79 %, respectively, which was higher than the binary spatio-temporal volume. In the final experiment, we used 2D affine moment invariants of the average image and 3D affine moment invariants of the new spatio-temporal volume. The resultant correct classification rate using the SVM and knn were 94 % and 90 %, respectively, which was the highest score in the series of the experiments. Table I shows the correct classification rate of our experiments.

Using the same database, Nixon et al. [11] used dynamic and static gait features to yield a feature vector. Static features include the body height, stride and heights of different body parts while dynamic features are the phase-weighted magnitudes of the Fourier frequencies for the hip and knee angular motions. The gait signature is derived using the adaptive forward floating search algorithm via selecting the features with higher discriminability values. They used the k-nearest neighbor rule as a classifier, and their system achieved a correct classification rate of 92 % using the leave-one-out cross validation rule. In their experiment they used 48 features for classification, on the other hand, we used 12 features. The comparison of their experiment and our experiment is shown in Table II.

B. Experiments with the divided volumes

For obtaining detailed features of the spatio-temporal volume, we divide the 3D volume into upper and lower volumes by threshold processing. We carried out four experiments, and the experimental conditions are as follows: (Exp. E) two volumes of the 3D binarized volume, (Exp. F) two volumes of the new 3D volume from differential images, (Exp. G) the 3D binarized volume and its divided volumes, and (Exp. H) the new spatio-temporal volume and two volumes of the 3D binarized volume. In these experiments, the 3D volume is divided into two volumes at two fifth from the bottom as show in Fig. 5, and the k-nearest neighbour classification was applied to the affine moment invariants as the classifier. The resultant correct classification rates in (Exp. E $\sim$ H) were 87 %, 84 %, 92 %, and 93 %, respectively. From these experiments, by dividing the full 3D volume into upper and lower volumes, more detailed features could be obtained than the full spatio-temporal volume.

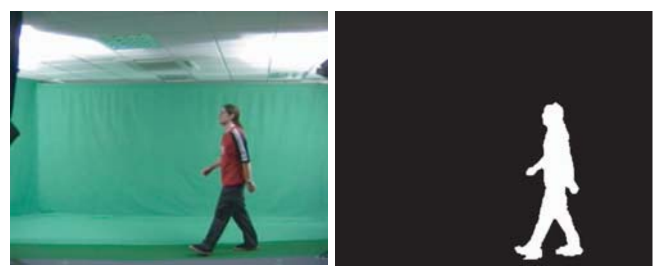

Fig. 3. Samples from the University of Southampton database. [21]

V. Conclusions

We proposed in this paper the person identification method using the hybrid biometric of physiological and behavioral biometrics, which is the full spatio-temporal volume carved by a person who walks. In addition to this biometric, its average image and new spatio-temporal volume, which was created from the average image and original images, were also considered as biometrics. We showed that affine moment invariants in conjunction with an SVM classifier may produce marginally better results than those based on gait analysis alone and k-nearest neighbour classification. Moreover, for obtaining detailed features of the sptaio-temporal volume, we extended the proposed method by dividing the 3D volume into upper and lower volumes. The calculation of the affine moment invariants is very straight forward, unlike the individual cues extracted to characterize gait and certain characteristics of the human body. In addition, the

TABLE I

THE CORRECT CLASSIFICATION RATE OF OUR EXPERIMENTS

Biometrics	The number of features	Correct classification rate [%]	
		SVM	knn
(Exp.A) 3D volume of binarized images	6	75	69
(Exp.B) Average images	6	92	89
(Exp.C) 3D volume of differential images	6	84	79
(Exp.D) Average images and 3D volume of differential images	12	94	90

TABLE II

COMPARISON OF THE EXPERIMENT OF [11] AND OUR EXPERIMENT

	The experiment of [11]	Our experiment
Classifier	The k-nearest neighbor rule	The support vector machine
Features	The gait signature consisting of 48 features	2D and 3D affine moment invariants consisting of 12 features
Classification rate [%]	92	94

affine moment invariants, being integrators, are more robust features than features based on differentiation.

One drawback may be that the spatio-temporal volumes we consider may be affected by clothing, so their use in unconstrained situations may not be robust. However, they may be used in conjunction with sensors that can "see through" clothing. Moreover, another limitation is the shape dependence on the viewing angle. To deal with this problem, the classifier can be trained by using the training data sets of different viewing angles. Finally, another drawback is that by the extended method, although the number of features is increased, it may ignore phase difference between the movement of arms and that of legs. However, from the experimental results, the proposed method is promising and merits further investigation.

VI. ACKNOWLEDGMENTS

The authors are grateful to Professor Maria Petrou (Imperial College London) for her helpful suggestions.

REFERENCES

[1] M.P. Murray, *Gait as a Total Pattern of Movement*, Am. J. Physical Medicine, vol. 46, no. 1, pp. 290-329, 1967.

[2] D. Cunado and M. Nixon and J. Carter, *Automatic Extraction and Description of Human Gait Models for Recognition Purposes*, CVIU, vol. 90, no. 1, pp. 1-41, 2003.

[3] C. Yam and M. Nixon and J. Carter, *Automated person recognition by walking and running via model-based approaches*, Pattern Recognition, vol. 37, no. 5, pp. 1057-1072, 2004.

[4] H. Murase and R. Sakai, *Moving object recognition in eigenspace representation: gait analysis and lip reading*, Pattern Recognition Letters, vol. 17, no. 2, pp. 155-162, 1996.

[5] S. Sarkar and P. Phillips and Z. Liu and I. Vega and P. Grother and K. Bowyer, *The humanID gait challenge problem: data sets, performance, and analysis*, IEEE Trans. PAMI, vol. 27, no. 2, pp. 162-177, 2005.

[6] J. Han and B. Bhanu, *Individual Recognition Using Gait Energy Image*, IEEE Trans. PAMI, vol. 28, no. 2, pp. 316-322, 2006.

[7] J. Little and J. Boyd, *Recognizing People by Their Gait: The Shape of Motion*, Videre, vol. 1, no. 2, pp. 1-32, 1998.

[8] J. Flusser and T. Suk, *Pattern recognition by affine moment invariants*, Pattern Recognition, vol. 26, no. 1, pp. 167-174, 1993.

[9] A. G. Mamistvalov, *n-Dimensional Moment Invariants and Conceptual Mathematical Theory of Recognition n-Dimensional Solids*, IEEE Trans. Pattern Analysis and Machine Intelligence, vol. 20, no. 8, pp. 819-831, 1998.

[10] M. Nixon and J. Carter, *Automatic Recognition by Gait*, Proc. the IEEE, vol. 94, no. 11, pp. 2013-2024, 2006.

[11] I. Bouchrika and M. Nixon,, *People Detection and Recognition using Gait for Automated Visual Surveillance*, Proc. IEE Inter. Symp. Imaging for Crime Detection and Prevention, 2006.

[12] R. Urtasun and P. Fua, *3D Tracking for Gait Characterization and Recognition*, Proc. 6th IEEE Int. Conf. Automatic Face and Gesture Recognition, pp. 17-22, 2004.

[13] L. Lee and W. Grimson, *Gait Analysis for Recognition and Classification*, Proc. IEEE Conf. Face and Gesture Recognition, pp.155-161, 2002.

[14] C. BenAbdelkader and R. Cutler and L. Davis, *Stride and Cadence as a Biometric in Automatic Person Identification and Verification*, Proc. IEEE Conf. Face and Gesture Recognition, pp. 372-377, 2002.

[15] R. Collins and R. Gross and J. Shi, *Silhouette-based human identification from body shape and gait*, IEEE Int. Conf. Automatic Face and Gesture Recognition, pp. 351-356, 2002.

[16] Z. Liu and S. Sarkar, *Improved Gait Recognition by Gait Dynamics Normalization*, IEEE Trans. Pattern Analysis and Machine Intelligence, vol. 28, no. 6, pp. 863-876, 2006.

[17] S. Niyogi and E. Adelson, *Analyzing and Recognizing Walking Figures in XYT*, IEEE Conf. Computer Vision and Pattern Recognition, pp. 469-474, 1994.

[18] Y. Liu and R. Collins and Y. Tsin, *Gait Sequence Analysis using Frieze Patterns*, Proc. the 7th European Conf. Computer Vision (ECCV'02), 2002.

[19] C. BenAbdelkader and R. Cutler and H. Nanda and L. Davis, *EigenGait: Motion-based Recognition of People using Image Self-Similarity*, 3rd Int. Conf. Audio- and Video-Based Biometric Person Authentication, 2001.

[20] D. Xu and H. Li, *3-D Affine Moment Invariants Generated by Geometric Primitives*, Proc. 18th IEEE Int. Conf. Pattern Recognition, pp. 544-547, 2006.

[21] J. D. Shutler and M. G. Grant and M. S. Nixon and J. N. Carter, *On a Large Sequence-Based Human Gait Database*, Proc. 4th Int. Conf. Recent Advances in Soft Computing, pp. 66-71, 2002.

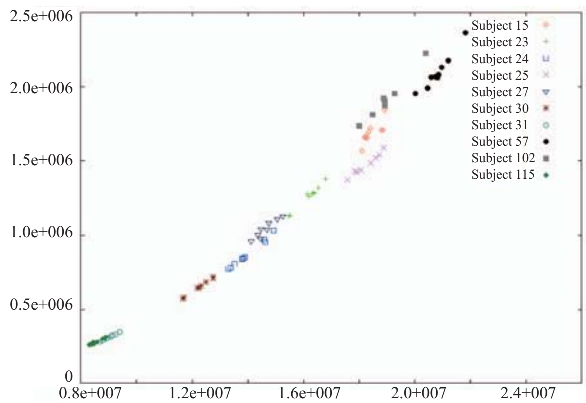

(a) Affine moment invariants

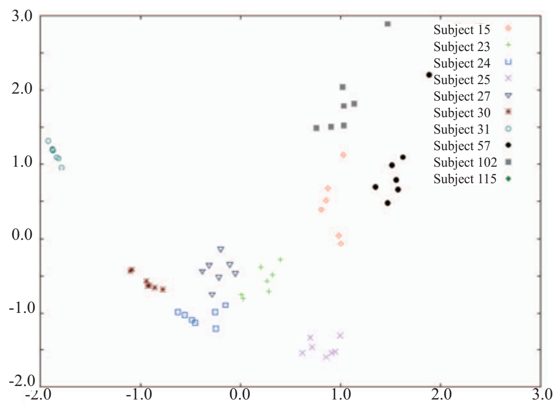

(b) Whitened affine moment invariants

Fig. 4. The first two affine moment invariants plotted against each other for 10 of the 20 subjects and their whitened values.

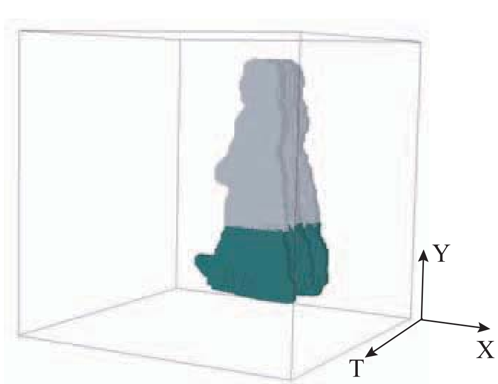

Fig. 5. Upper and lower volumes.